J Membrane Biol (2014) 247:461–468
DOI 10.1007/s00232-014-9647-y

ORIGINAL ARTICLES

Phosphoinositide 3-Kinase Pathway Mediates Early Aldosterone Action on Morphology and Epithelial Sodium Channel in Mammalian Renal Epithelia

Yuan Zhou · Xuewei Chen · Xiao Liu · Hujie Lu · Ying Li · Hui Zhu · Gaihong An · Na Zhang · Jianning Zhang · Qiang Ma · Yanjun Zhang

Received: 20 November 2013 / Accepted: 25 February 2014 / Published online: 11 April 2014

Abstract Involvement of phosphoinositide 3-kinases (PI3Ks) in early aldosterone action on epithelial sodium channel (ENaC) in mammalian renal epithelia was investigated by hopping probe ion conductance microscopy combined with patch-clamping in this study. Aldosterone treatment enlarged the cell volume and elevated the apical membrane of renal mpkCCDc14 epithelia, which resulted in enhancing the open probability of ENaC. Inhibition of PI3K pathway by LY294002 obviously suppressed these aldosterone-induced changes in both cell morphology and ENaC activity. These results indicated the important role of PI3K pathway in early aldosterone action and the close relationship between cell morphology and ENaC activity in mammalian renal epithelia.

Keywords ENaC · CCD · HPICM · SICM · PI3K

Yuan Zhou and Xuewei Chen contributed equally to this work.

Y. Zhou · Y. Li · H. Zhu · J. Zhang (✉) · Y. Zhang (✉)
Department of Neurosurgery, Tianjin Medical University General Hospital; Tianjin Neurological Institute; Key Laboratory of Post-trauma Neuro-repair and Regeneration in Central Nervous System, Ministry of Education; Tianjin Key Laboratory of Injuries, Variations and Regeneration of Nervous System, 154 Anshan Road, Heping District, Tianjin 300052, China
e-mail: jianningzhang@hotmail.com

Y. Zhang
e-mail: yanjun_zhang@hotmail.com

X. Chen · G. An · N. Zhang · Q. Ma (✉)
Department of Occupational Hygiene, Institute of Health and Environmental Medicine, 1 Dali Road, Heping District, Tianjin 300050, China
e-mail: maqiangw@sina.com

X. Liu · H. Lu · Y. Zhang
Nanomedicine Laboratory, China National Academy of Nanotechnology & Engineering, TEDA, Tianjin 300457, China

Y. Zhang
Medicine Division, Imperial College London, London W12 0NN, UK

Introduction

Epithelial sodium channel (ENaC) is crucial to regulate blood pressure, and performs a rate-limiting step for Na^+ reabsorption in renal epithelia (Garty and Palmer 1997). Activity of ENaC is tightly modulated by aldosterone in renal cortical-collecting duct (CCD) (Eaton et al. 2001; Palmer et al. 2012). There are two possible ways to increase Na^+ reabsorption in response to aldosterone, namely, by augmenting numbers and/or by enhancing the open probability (P_o) of ENaCs (Palmer et al. 2012; Rossier 2003). Early effects of aldosterone can increase Na^+ reabsorption within 3 h before significant increase in protein expression of ENaCs (Garty and Palmer 1997; May et al. 1997), suggesting that early aldosterone action on ENaC activity may mainly result from the increased channel P_o (Eaton et al. 2001; Palmer et al. 2012; Kemendy et al. 1992). Although many studies focus on such early aldosterone action on ENaC activity, more regulation mechanisms remain to be learned in mammalian renal epithelia (Dooley et al. 2012).

Some studies indicated that phosphoinositide 3-kinase (PI3K) pathway was required for aldosterone actions on Na^+ transport by increasing the P_o of ENaCs (Staruschenko et al. 2004, 2007; Blazer-Yost et al. 1999). Aldosterone stimulated the activity of PI3K and consequently promoted the synthesis of its downstream products PtdIns(3,4,5)P_3 (PIP_3) (Blazer-Yost et al. 1999), which was suggested to stimulate ENaC activity directly (Pochynyuk

et al. 2008; Helms et al. 2005; Ma et al. 2001; Tong et al. 2004; Pochynyuk et al. 2005). PI3K pathway was also known to be strongly involved in the reorganization of cell actin cytoskeleton (Carpenter and Cantley 1996), which had been demonstrated to regulate the cell morphology (Ivanov et al. 2010) and the P_o of ENaC (Cantiello 1995; Berdiev et al. 1996). Our previous study also showed that PI3K pathway played important roles in aldosterone early action on ENaC activity and cell morphology in *Xenopus* renal epithelia A6 cells (Gorelik et al. 2005). However, little is known about the correlation between the ENaC activity and the cell morphology to respond to the aldosterone in a PI3K-signaling-modulated manner in living mammalian CCD epithelia.

In this study, with the help of a combination of patch-clamp and high-resolution noncontact hopping probe ion conductance microscopy (HPICM) (Novak et al. 2009; Yang et al. 2011), we further investigated the involvement of PI3K pathway in the early aldosterone action on ENaC activity and cell morphology in mouse CCD mpkCCDc14 cells (Bens et al. 1999).

Methods

Reagents

DMEM/F12 (1:1) medium was purchased from Thermo Scientific Hyclone (Beijing, China). Heat-inactivated fetal bovine serum (FBS) was bought from ExCell Biology (Shanghai, China). L15 medium, Insulin–Transferrin–Selenium, penicillin, and streptomycin were bought from Gibco (Langley, OK, USA). Glucose monohydrate, 3,3′,5-Triiodo-L-thyronine sodium salt (T3), Dexamethasone, LY294002, aldosterone, and amiloride were purchased from Sigma-Aldrich (St. Louis, MO, USA). Murine EGF was bought from PeproTech Inc. (Rocky Hill, NJ, USA). HEPES buffer was purchased from Amresco LLC (Cochran Road, Solon, USA).

Cell Culture

Mouse CCD mpkCCDc14 cell line was provided as a generous gift by Prof. Zhiren Zhang (Medical University of Harbin, China) and cultured as per previously published methods (Bens et al. 1999; Chen et al. 2013). In brief, cells were cultured in the growth medium DMEM/F12 (1:1) with 2 g/L Glucose monohydrate, 100 μg/mL streptomycin, and 100 U/mL penicillin; and supplemented with 1 % (V/V) Insulin–Transferrin–Selenium, 0.5 mM Dexamethasone, 1 μM T3, 10 μg/mL EGF, and 2 % FBS at 37 °C in a humidified 5 % CO_2 atmosphere. Cells were passaged twice a week with the medium being changed every 2 days.

For experiments, cells were seeded on cell culture inserts (0.4-μm pore size on Polyethylene terephthalate membrane; BD Biosciences, Durham, USA) at a density of 1×10^5 cells/well and grown for 10–12 days to form a polarized epithelial monolayer (Kemendy et al. 1992; Gorelik et al. 2005). Then, mpkCCDc14 cells were pretreated with aldosterone using a modified protocol reported by Kemendy et al. 1992. In brief, the mature mpkCCDc14 cell monolayer was maintained for 24 h in the growth medium supplemented with 2 % FBS and 1 μm aldosterone. After 24 h, the cell monolayer was incubated in a serum-free medium but only with aldosterone for a further 24 h. The cells were then grown in a culture medium free of both serum and aldosterone for the final duration of 24–48 h.

Transepithelial Electrical Resistance (TEER) Measurements

Transepithelial electrical resistance (TEER) measurements of mpkCCDc14 cell monolayer were investigated by a commercial epithelial volt ohmmeter (EVOM, World Precision Instruments, USA) and an ENDOHM-24 SNAP Chamber (World Precision Instruments, USA) as per previously published methods (Zhang et al. 2005). In brief, TEER measurements were performed in the L15 medium at 37 °C after the EVOM reading became stable (~30 min). Only monolayers with a stable initial TEER of greater than 4,000 Ω cm^2 were chosen for the experiments. In order to determine whether any observed effects involved the ENaC activity, 10 μM ENaC inhibitor amiloride was added to the apical side of the cell monolayer to induce an amiloride-sensitive part of TEER measurement.

Hopping Probe Ion Conductance Microscopy (HPICM) Imaging of Living mpkCCDc14 Cell Monolayer

The HPICM (Ionscope Ltd., UK) was set up as described previously (Novak et al. 2009; Yang et al. 2011, 2012). In brief, a HPICM probe was mounted on a 3D piezoelectric translation stage. The HPICM probe consists of a glass pipette filled with the L15 medium and plugged into an Ag/AgCl electrode. An external Axon MultiClamp 700B amplifier and a Digidata 1440A analog-to-digital converter (Molecular Devices, USA) were used to monitor the ion current passing through the probe and supply a DC voltage of 200 mV between pipette electrode and bath electrode. At each imaging point, the probe approached the mpkCCDc14 cell from a starting position, and the reference ion current was measured, while the probe was well above the cell surface. The probe then approached until the ion currents were reduced by 0.4 %, and the position of

z-dimensional piezo was recorded as the height of the cell at this imaging point. The data acquisition electronics recorded both the lateral and vertical positions of the probe, which then can be used to generate the topographical image of living mpkCCDc14 epithelia.

HPICM scanning pipettes were pulled from borosilicate glasses (O.D. 1.00 mm, I.D. 0.59 mm, VitalSense Scientific Instruments Co., China) using a laser-based puller, Model P-2000 (Sutter Instruments Co., USA). The resistance of scanning pipettes was $\sim$100 MΩ. Both the pipette solution and bath solution were of L15 medium. The time required to scan a 50 × 50 μm area with a typical resolution of 128 × 128 pixels was about 20 min, while it was15 min for a 30 × 30 μm scanning. All HPICM experiments were carried out at the room temperature (24 ± 2 °C).

Patch-Clamp Recording

Ion channel currents were recorded with the cell-attached configuration of patch-clamp technique, using a MultiClamp 700B amplifier connected with a Digidata 1440A analog-to-digital converter (Molecular Devices, USA) (Yang et al. 2011, 2012). HPICM scanning pipette was precisely controlled by HPICM piezo stage to approach to the cell surface. When a gigaohm seal was formed, successive ion channel activities were recorded. Evoked currents were sampled at 10 kHz and low-pass filtered at 1 kHz by an eight-pole Bessel filter. The resistance of patch-clamp pipettes was 6–10 MΩ. Patch-clamp pipette solution was the same as bath solution (in mM): 145 NaCl, 5 KCl, 1 $CaCl_2$, 1 $MgCl_2$, and 10 HEPES (pH 7.4). All Patch-clamp recordings were performed at the room temperature (24 ± 2 °C).

Data Processing and Statistical Analysis

The HPICM images were processed and analyzed by means of SICM Image Viewer software (Ionscope Ltd, UK). The ion channel recordings were analyzed using pClamp10.2 (Molecular Device, CA, USA) and Origin 8.0 software (Originlab Corporation, USA). Values were presented as mean ± SEM. Statistical significance was determined by the Student's t test. A difference between means at level of $P < 0.05$ was considered statistically significant; $P < 0.005$ was statistically highly significant.

Results

Early Aldosterone Action on Amiloride-Sensitive Transepithelial Electrical Resistance (TEER) in mpkCCDc14 Cell Monolayer

Similar to those previously published results (Bens et al. 1999; Wang et al. 2008), 1 μM aldosterone treatment significantly increased the absolute value of amiloride-sensitive transepithelial electrical resistance (TEER) of cell monolayer within 3 h (Fig. 1a), which was accompanied by the TEER reduction in whole mpkCCDc14 cell monolayer. This result indicated that early aldosterone action increased the ENaC activities of whole mpkCCDc14 cell monolayer.

To evaluate the involvement of PI3K pathway in early aldosterone action, the mpkCCDc14 cells were pretreated with PI3K pathway inhibitor LY294002 for 30 min before any aldosterone stimulation (Fig. 1b). It showed clearly that the inhibition of PI3Ks completely blocked the effects of aldosterone on the transepithelial Na^+ transport of mpkCCDc14 cell monolayer. Similarly, LY294002 inhibition effects on Na^+ transport were also observed by other research teams (Staruschenko et al. 2007; Wang et al. 2008).

Early Aldosterone Action on Cell Morphology and ENaC Activity of mpkCCDc14 Cells

The relationship between the aldosterone-induced cell morphological change and ENaC activity in mpkCCDc14 cell was investigated by HPICM combined with patch-clamp. As a control experiment, mpkCCDc14 cell monolayer was continuously observed with HPICM (Fig. 2). Figure 2a presents five time-lapse images of a chosen 50 × 50 μm^2 area of control mpkCCDc14 cell monolayer taken over a 3-h period. Neither HPICM topographical images of mpkCCDc14 cell monolayer (Fig. 2a) nor scanning profiles of solid-line-marked cells (Fig. 2b) showed any visible changes in cell morphology during 3-h HPICM scanning.

Figure 3a presents another series of HPICM images of aldosterone-treated mpkCCDc14 cell monolayer taken over a 3-h period. The mpkCCDc14 cells morphology presented two visible change trends: changed morphology (Figure 3a, high-lighted cells with numbers of 1–3) and non-changed morphology (Fig. 3a, cell marked with *). These aldosterone-induced morphology-changed mpkCCDc14 cells were recruited progressively within 3 h, and the percentage of morphology-changed cells was about 55 % after 3-h aldosterone exposure. With the help of previously published measurement methods for cell height and cell volume (Korchev et al. 2000), we calculated these morphology-changed cells and found that aldosterone treatment increased the average values of cell height and cell volume by about 1 μm and 268 μm^3, respectively. These morphological changes were demonstrated more clearly by HPICM scanning profiles of those solid-line-marked cells (Fig 3b). The bottom black scanning profile represents the solid-line-highlighted three cells in the control frame of Fig. 3a. The blue scanning profile shows the dramatic apical membrane elevations of these cells after 3-h aldosterone stimulation.

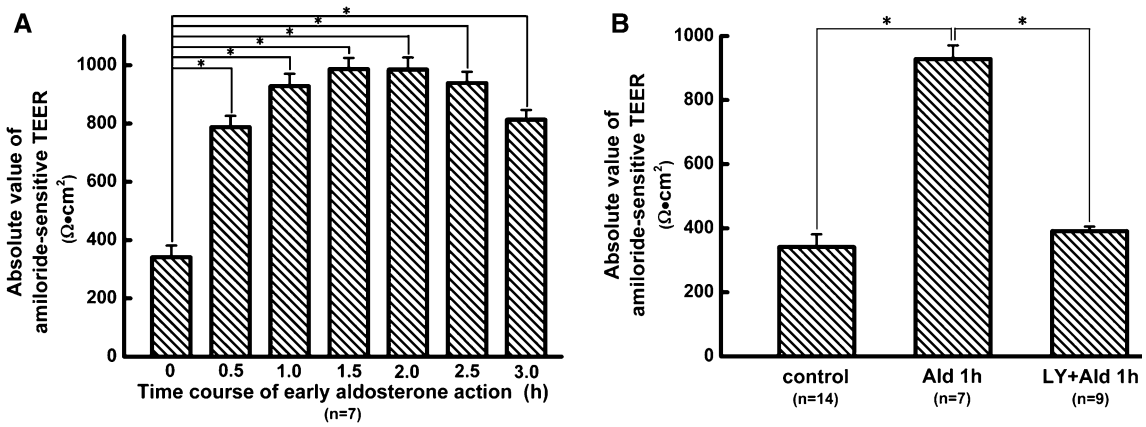

Fig. 1 Absolute value of amiloride-sensitive TEER measurements of mpkCCDc14 cell monolayer. **a** Histogram showing the time courses of early aldosterone (Ald) effects on the absolute value of amiloride-sensitive TEER changes of mpkCCD cell monolayer. **b** Histogram showing the effects of PI3K inhibitor LY294002 (LY) on the absolute value of amiloride-sensitive TEER of mpkCCDc14 cell monolayer

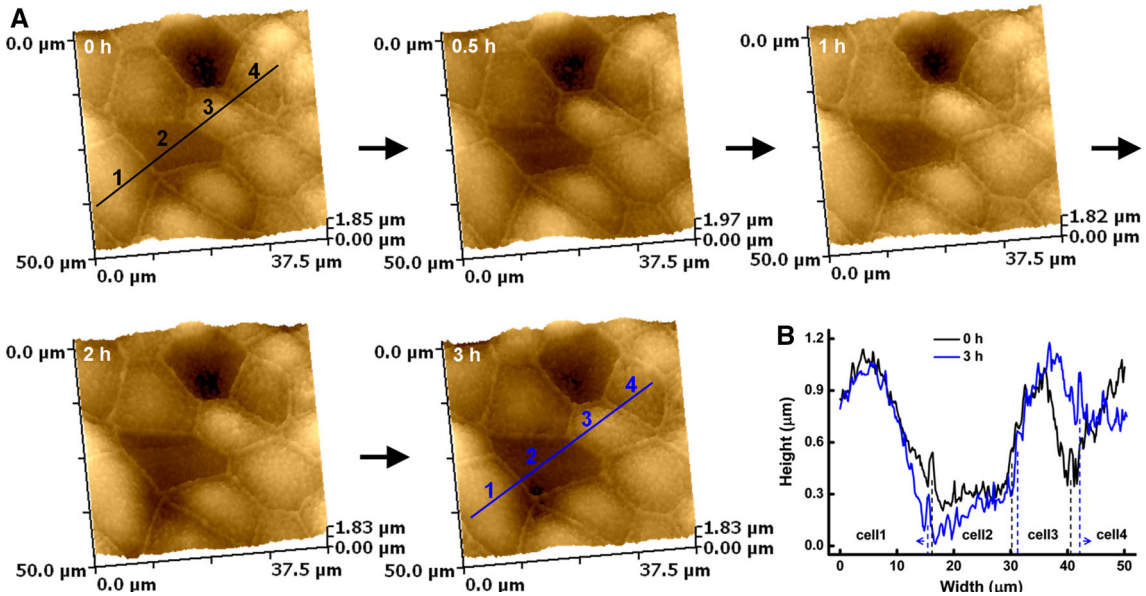

Fig. 2 HPICM images of a live mpkCCDc14 cell monolayer. **a** Five images chosen from a sequence of 3-h time-lapse scanning of a selected 50 × 50 μm area in mpkCCDc14 cell monolayer. The time in hours from the start of the experiment is shown for *each image*. **b** Time-dependent scanning profile changes of the solid line via cells *marked 1–4* in **a**. *Black trace* from control "0 h" frame, *blue trace* from "3 h" frame

In order to detect the link between ENaC activity and aldosterone-induced cell morphology changes, HPICM combined with patch-clamp was utilized on those morphology-changed (Fig. 4a) and nonchanged mpkCCDc14 cells (Fig. 4b) (Chen et al. 2013), respectively. Electric current traces from cell-attached recordings indicated that aldosterone treatment significantly increased the ENaC P_o of morphology-changed cells from 0.18 ± 0.04 to 0.35 ± 0.05 ($P < 0.005$, Fig. 4c). However, such aldosterone-induced changes in ENaC activity were not recorded from those morphology-nonchanged mpkCCDc14 cells (Fig. 4c). Single-channel conductances of both the morphology-changed and the nonchanged mpkCCDc14 cells were about 4.95 ± 0.06 pS (Fig. 4d), which was characterized to be ENaC channel property as published previously (Staruschenko et al. 2007; Gorelik et al. 2005).

Involvement of PI3K Pathway in the Early Aldosterone Action on Cell Morphology Changes and ENaC Activities of mpkCCDc14 Cell

In order to investigate the involvement of PI3K pathway in the aldosterone action on the cell morphology and ENaC activity of mpkCCDc14 cells, HPICM combined with

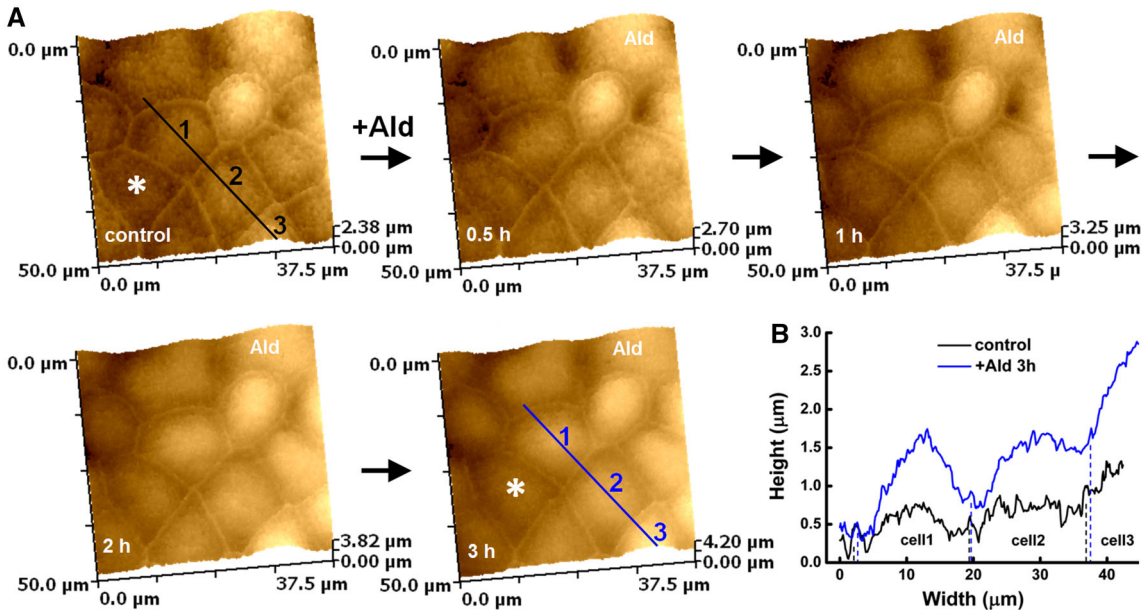

Fig. 3 Aldosterone effects on the changes in cell morphology of mpkCCDc14 cells. **a** Five images chosen from a sequence of 3-h time-lapse scanning of a selected 50 × 50 μm area in mpkCCDc14 cell monolayer. The time in hours from the start of the experiment is shown for each image. **b** Time-dependent profile changes of the solid line via cells *marked 1–3* in **a**. *Black trace* from control "0-h" frame; *blue trace* from "3-h" frame (Color figure online)

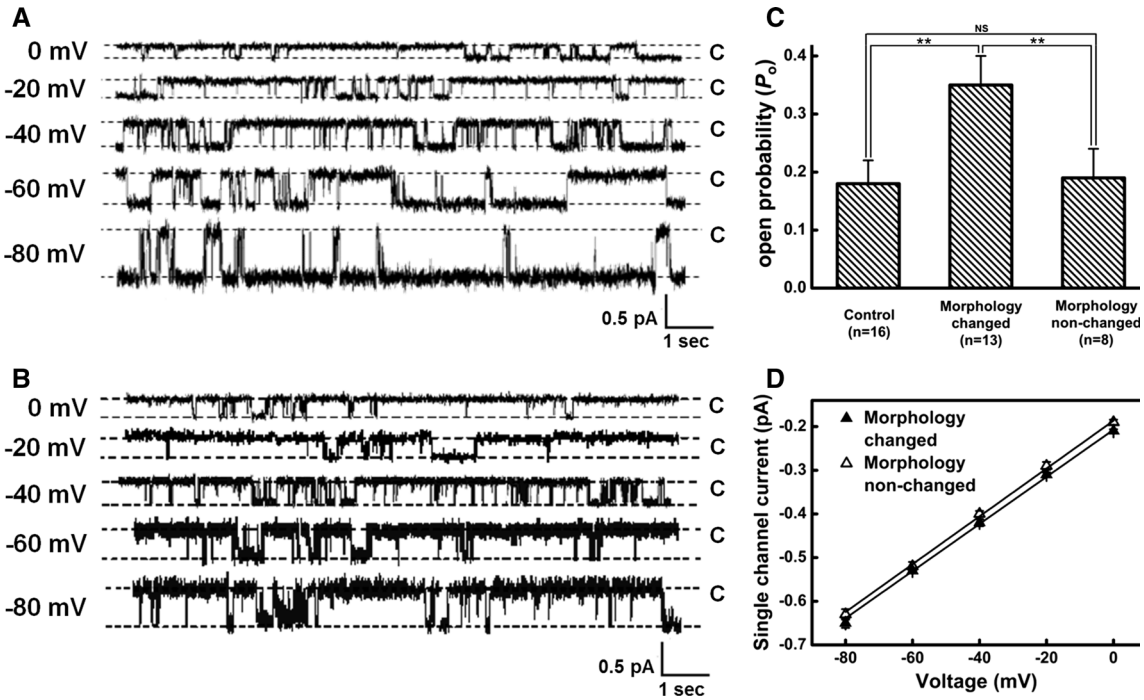

Fig. 4 Ion-channel activities of aldosterone-treated mpkCCDc14 cells. **a** Ion current traces from a representative cell-attached recording made on the apical membrane of aldosterone-treated morphology-changed mpkCCDc14 cell. **b** A set of ion current traces from a cell-attached patch-clamp on the apical membrane of aldosterone-treated morphological-nonchanged mpkCCDc14 cell. **c** Calculated means of ion-channel open probability (P_o) of mpkCCDc14 cells in the groups of control, the aldosterone-induced morphology-changed, and nonchanged mpkCCDc14 cells. **d** Current–voltage (I–V) relation for single ion-channel of aldosterone-induced morphology-changed and morphology-nonchanged mpkCCDc14 cells

patch-clamp was utilized again (Fig. 5). Two chosen topographical images from a series of HPICM scanning of mpkCCDc14 cell monolayer are presented in Fig. 5a. The control image was taken before any stimulation, and it showed the expected features of intact mpkCCDc14 cell monolayer. Pretreatment with PI3K inhibitor LY294002

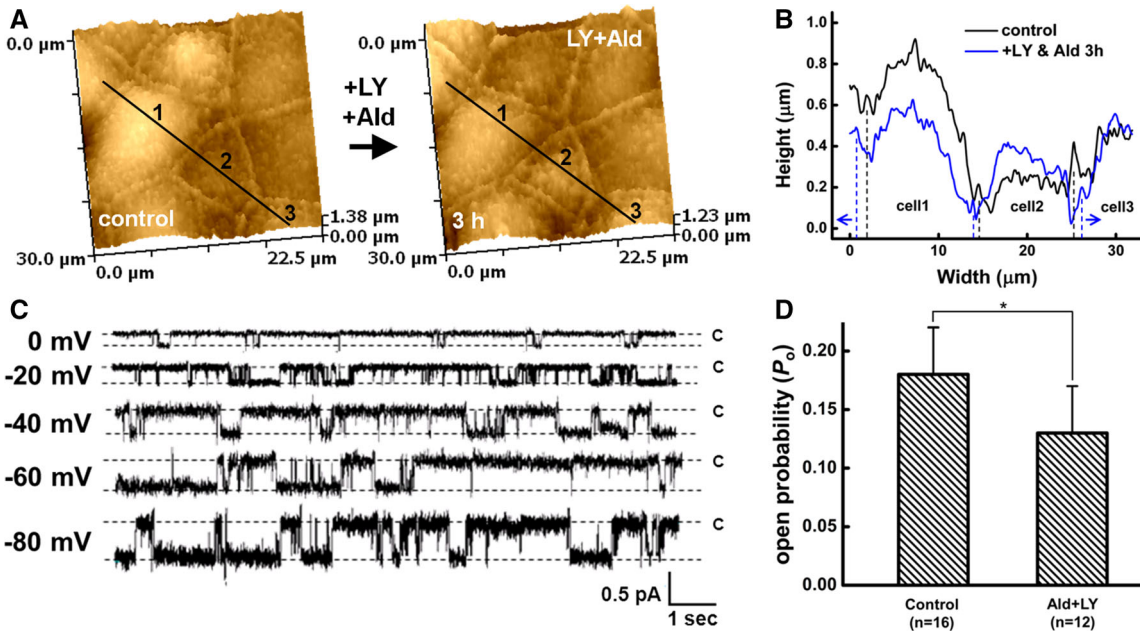

Fig. 5 Effects of LY294002 (LY) on aldosterone-induced changes in cell morphology and ENaC activity of mpkCCDc14 cells. **a** Two images chosen from a sequence scannings of 3-h time-lapse scanning of a selected 30 × 30 µm area of a LY294002 (LY)-pretreated mpkCCDc14 cell monolayer in response to aldosterone (Ald) stimulation. **b** Time-dependent scanning profile changes of the solid line via cells *marked 1–3* in **a**. **c** Current traces from apical membrane of aldosterone-induced morphology-changed mpkCCDc14 monolayer after the treatment with LY. **d** Calculated mean open probability of ENaC of mpkCCDc14 cells in the groups of control and Ald+LY

for 0.5 h inhibited the previously observed aldosterone-induced cell morphology changes, which even decreased the cell height and the cell volume by about 0.2 µm and 20 µm^3, respectively (Fig. 5a, b). Compared with patch-clamp recordings obtained from control cells, pretreatment with PI3K inhibitor not only inhibited the previously observed aldosterone-induced increasing in ENaC P_o, but also significantly reduced ENaC P_o to about 0.13 ± 0.04 ($p < 0.05$, Fig. 5d). Such PI3K inhibition that abolished aldosterone action on ENaC activity was similar to the previously published results (Staruschenko et al. 2007).

Discussion

In aldosterone-responsive renal epithelia, ENaC plays a critical role in modulating homeostasis of Na^+, blood volume, and thus, chronic blood pressure (Garty and Palmer 1997; Eaton et al. 2001; Palmer et al. 2012). The regulation of ENaC activity by early aldosterone action has been intensively studied in amphibian renal epithelial cells (Gorelik et al. 2005), but relatively little information exists regarding the modulation mechanisms in mammalian CCD. With the help of HPICM combined with patch-clamp technique and TEER measurement, we found that early aldosterone action induced time-dependent morphological changes in about 55 % of mpkCCDc14 cells and increased amiloride-sensitive Na^+ currents of whole cell monolayer within 3 h, which were similar to our previously observations in amphibian A6 cells (Gorelik et al. 2005; Zhang et al. 2007). It is suggested that aldosterone may enhance the release of ATP from some renal epithelial cells and activate the basolateral purinergic receptors of their adjacent cells to produce rapid morphology/volume changing, as we have described previously (Gorelik et al. 2005; Zhang et al. 2007). However, further investigation on such involvement of aldosterone and purinergic signaling in mammalian CCD cells needs to be done in the future. In this study, patch-clamp recordings of individual aldosterone-treated mpkCCDc14 cell, which enabled the morphology and physiological function to be correlated, showed that the morphology of mpkCCDc14 cells changed with the increase in ENaC activities. Moreover, an extensive body of literature (Staruschenko et al. 2004, 2007; Blazer-Yost et al. 1999; Pochynyuk et al. 2008; Helms et al. 2005; Ma et al. 2001; Tong et al. 2004; Pochynyuk et al. 2005; Gorelik et al. 2005) indicates that PI3K is a crucial signaling pathway for aldosterone action. Although PI3K is not an aldosterone-induced protein, its activity is regulated by aldosterone in renal epithelia to produce PIP_3 (Blazer-Yost et al. 1999; Helms et al. 2005), which can enhance the P_o of ENaC directly (Pochynyuk et al. 2008; Helms et al. 2005; Ma et al. 2001; Tong et al. 2004; Pochynyuk et al. 2005). Our observed aldosterone-induced

changes in cell morphology, trans-epithelial Na^+ transport, and ENaC activities were markedly blocked by PI3Ks inhibitor LY294002. It is tempting to conclude that aldosterone that activates PI3K pathway, which induces change in the anatomy of those cells that responded, can trigger the activity of the apical ENaC in mammalian renal CCD.

ENaCs have been reported to be activated by cell morphological changes during swelling (hypotonic stress) and be suppressed by cell morphological changes during shrinkage (hypertonic stress), which were mediated via actin filament depolymerization and consequently regulated the P_o of ENaC (Awayda and Subramanyam 1998). Downstream effectors of PIP_3 in PI3K pathway are thought to stimulate actin polymerization and drive changes in membrane morphology (Chen et al. 2012). Such PI3K involving regulation of cell morphology may also participate in the mechanical force (membrane stretch)-regulated activation of ENaC (Rozansky et al. 2002; Fronius and Clauss 2008; Althaus et al. 2007).

It is likely that PI3K pathway is also integral to increases in Na^+ transport in response to IGF, insulin, hydrogen peroxide, or hypotonic stress in renal epithelial cells (Fronius and Clauss 2008; Record et al. 1998; Paunescu et al. 2000; Ma 2011). Given the need for rapid and dynamic modulation of Na^+ reabsorption, it is not surprising that ENaC activity can be regulated via PI3K pathway to integrate different stimuli and a variety of intrinsic factors. We observed that aldosterone acutely enhanced change of cell morphology and ENaC activity involving PI3K pathway is important in regulating ENaC function, which not only demonstrates that HPICM combined with patch-clamp technique is a powerful physiological research tool, but also supports the potential for targeting PI3K as a therapeutic approach for hypertension.

Acknowledgments This work was supported by the National Natural Science Foundation of China (No.30971184; 81271361; 81330029; 31300828), the International Science & Technology Cooperation Program of China (No.2011DFG33430), and Tianjin Natural Science Foundation of China (No.13JCYBJC21900; 12JCYBJC31500).

Conflict of interest There are no conflicts of interest.

References

Althaus M, Bogdan R, Clauss WG, Fronius M (2007) Mechano-sensitivity of epithelial sodium channels (ENaCs): laminar shear stress increases ion channel open probability. FASEB J 21:2389–2399

Awayda MS, Subramanyam M (1998) Regulation of the epithelial Na^+ channel by membrane tension. J Gen Physiol 112:97–111

Bens M, Vallet V, Cluzeaud F, Pascual-Letallec L, Kahn A, Rafestin-Oblin ME, Rossier BC, Vandewalle A (1999) Corticosteroid-dependent sodium transport in a novel immortalized mouse collecting duct principal cell line. J Am Soc Nephrol 10:923–934

Berdiev BK, Prat AG, Cantiello HF, Ausiello DA, Fuller CM, Jovov B, Benos DJ, Ismailov II (1996) Regulation of epithelial sodium channels by short actin filaments. J Biol Chem 271:17704–17710

Blazer-Yost BL, Päunescu TG, Helman S, Lee KD, Vlahos CJ (1999) Phosphoinositide 3-kinase is required for aldosterone-regulated sodium reabsorption. Am J Physiol 277:C531–C536

Cantiello HF (1995) Role of the actin cytoskeleton on epithelial Na^+ channel regulation. Kidney Int 48:970–984

Carpenter CL, Cantley LC (1996) Phosphoinositide kinases. Curr Opin Cell Biol 8:153–158

Chen CL, Wang Y, Sesaki H, Iijima M (2012) Myosin I links PIP3 signaling to remodeling of the actin cytoskeleton in chemotaxis. Sci Signal 5:ra10

Chen X, Zhu H, Liu X, Lu H, Li Y, Wang J, Liu H, Zhang J, Ma Q, Zhang Y (2013) Characterization of two mammalian cortical collecting duct cell lines with hopping probe ion conductance microscopy. J Membr Biol 246:7–11

Dooley R, Harvey BJ, Thomas W (2012) Non-genomic actions of aldosterone: from receptors and signals to membrane targets. Mol Cell Endocrinol 350:223–234

Eaton DC, Malik B, Saxena NC, Al-Khalili OK, Yue G (2001) Mechanisms of aldosterone's action on epithelial Na^+ transport. J Membr Biol 184:313–319

Fronius M, Clauss WG (2008) Mechano-sensitivity of ENaC: may the (shear) force be with you. Pflug Arch 455:775–785

Garty H, Palmer LG (1997) Epithelial sodium channels: function, structure, and regulation. Physiol Rev 77:359–396

Gorelik J, Zhang Y, Sánchez D, Shevchuk A, Frolenkov G, Lab M, Klenerman D, Edwards C, Korchev Y (2005) Aldosterone acts via an ATP autocrine/paracrine system: the Edelman ATP hypothesis revisited. Proc Natl Acad Sci USA 102:15000–15005

Helms MN, Liu L, Liang YY, Al-Khalili O, Vandewalle A, Saxena S, Eaton DC, Ma HP (2005) Phosphatidylinositol 3,4,5-trisphosphate mediates aldosterone stimulation of epithelial sodium channel (ENaC) and interacts with gamma-ENaC. J Biol Chem 280:40885–40891

Ivanov AI, Parkos CA, Nusrat A (2010) Cytoskeletal regulation of epithelial barrier function during inflammation. Am J Pathol 177:512–524

Kemendy AE, Kleyman TR, Eaton DC (1992) Aldosterone alters the open probability of amiloride-blockable sodium channels in A6 epithelia. Am J Physiol 263:C825–C837

Korchev YE, Gorelik J, Lab MJ, Sviderskaya EV, Johnston CL, Coombes CR, Vodyanoy I, Edwards CR (2000) Cell volume measurement using scanning ion conductance microscopy. Biophys J 78:451–457

Ma HP (2011) Hydrogen peroxide stimulates the epithelial sodium channel through a phosphatidylinositide 3-kinase-dependent pathway. J Biol Chem 286:32444–32453

Ma HP, Saxena S, Warnock DG (2001) Anionic phospholipids regulate native and expressed epithelial sodium channel (ENaC). J Biol Chem 277:7641–7644

May A, Puoti A, Gaeggeler HP, Horisberger JD, Rossier BC (1997) Early effect of aldosterone on the rate of synthesis of the epithelial sodium channel alpha subunit in A6 renal cells. J Am Soc Nephrol 8:1813–1822

Novak P, Li C, Shevchuk AI, Stepanyan R, Caldwell M, Hughes S, Smart TG, Gorelik J, Ostanin VP, Lab MJ, Moss GW, Frolenkov GI, Klenerman D, Korchev YE (2009) Nanoscale live-cell imaging using hopping probe ion conductance microscopy. Nat Methods 6:279–281

Palmer LG, Patel A, Frindt G (2012) Regulation and dysregulation of epithelial Na^+ channels. Clin Exp Nephrol 16:35–43

Paunescu TG, Blazer-Yost BL, Vlahos CJ, Helman SI (2000) LY-294002-inhibitable PI 3-kinase and regulation of baseline rates

of Na(+) transport in A6 epithelia. Am J Physiol Cell Physiol 279:C236–C247

Pochynyuk O, Staruschenko A, Tong Q, Medina J, Stockand JD (2005) Identification of a functional phosphatidylinositol 3,4,5-trisphosphate binding site in the epithelial Na^+ channel. J Biol Chem 280:37565–37571

Pochynyuk O, Bugaj V, Stockand JD (2008) Physiologic regulation of the epithelial sodium channel by phosphatidylinositides. Curr Opin Nephrol Hypertens 17:533–540

Record RD, Froelich LL, Vlahos CJ, Blazer-Yost BL (1998) Phosphatidylinositol 3-kinase activation is required for insulin-stimulated sodium transport in A6 cells. Am J Physiol 274:E611–E617

Rossier BC (2003) The epithelial sodium channel (ENaC): new insights into ENaC gating. Pflug Arch 446:314–316

Rozansky DJ, Wang J, Doan N, Purdy T, Faulk T, Bhargava A, Dawson K, Pearce D (2002) Hypotonic induction of SGK1 and Na^+ transport in A6 cells. Am J Physiol Renal Physiol 283:F105–F113

Staruschenko A, Patel P, Tong Q, Medina JL, Stockand JD (2004) Ras activates the epithelial Na(+) channel through phosphoinositide 3-OH kinase signaling. J Biol Chem 279:37771–37778

Staruschenko A, Pochynyuk O, Vandewalle A, Bugaj V, Stockand JD (2007) Acute regulation of the epithelial Na^+ channel by phosphatidylinositide 3-OH kinase signaling in native collecting duct principal cells. J Am Soc Nephrol 18:1652–1661

Tong Q, Gamper N, Medina JL, Shapiro MS, Stockand JD (2004) Direct activation of the epithelial Na^+ channel by phosphatidylinositol 3,4,5-trisphosphate and phosphatidylinositol 3,4-bisphosphate produced by phosphoinositide 3-OH kinase. J Biol Chem 279:22654–22663

Wang J, Knight ZA, Fiedler D, Williams O, Shokat KM, Pearce D (2008) Activity of the p110-subunit of phosphatidylinositol-3-kinase is required for activation of epithelial sodium transport. Am J Physiol Renal Physiol 295:F843–F850

Yang X, Liu X, Zhang X, Lu H, Zhang J, Zhang Y (2011) Investigation of morphological and functional changes during neuronal differentiation of PC12 cells by combined hopping probe ion conductance microscopy and patch-clamp technique. Ultramicroscopy 111:1417–1422

Yang X, Liu X, Lu H, Zhang X, Ma L, Gao R, Zhang Y (2012) Real-time investigation of acute toxicity of ZnO nanoparticles on human lung epithelia with hopping probe ion conductance microscopy. Chem Res Toxicol 25:297–304

Zhang Y, Gorelik J, Sanchez D, Shevchuk A, Lab M, Vodyanoy I, Klenerman D, Edwards C, Korchev Y (2005) Scanning ion conductance microscopy reveals how a functional renal epithelial monolayer maintains its integrity. Kidney Int 68:1071–1077

Zhang Y, Sanchez D, Gorelik J, Klenerman D, Lab M, Edwards C, Korchev Y (2007) Basolateral P2X4-like receptors regulate the extracellular ATP-stimulated epithelial Na^+ channel activity in renal epithelia. Am J Physiol Renal Physiol 292:F1734–F1740